A Theoretical Study of Oxygen Atom Transfer Reactions from Oxiranes to Heavy Carbenes

Ming-Der Su

School of Chemistry, Kaohsiung Medical University, Kaohsiung 80708, Taiwan, Republic of China

Received: May 9, 2002; In Final Form: August 13, 2002

The potential energy surfaces for the abstraction reactions of heavy carbenes with oxirane have been studied using density functional theory (B3LYP). Five carbene species, including methylene, CH_2; silylene, SiH_2; germylene, GeH_2; stannylene, SnH_2; and plumbylene, PbH_2; have been chosen in this work as model reactants. The present theoretical investigations suggest that the relative carbenic reactivity decreases in the order: $CH_2 > SiH_2 > GeH_2 \gg SnH_2 > PbH_2$. That is to say, for oxirane deoxygenations, there is a very clear trend toward higher activation barriers and more endothermic (or less exothermic) reactions on going from C to Pb. More specifically, the theoretical findings strongly suggest that CH_2, SiH_2, and GeH_2 should readily abstract oxygen atoms from oxiranes, while SnH_2 and PbH_2 are unreactive with oxiranes. Furthermore, a configuration mixing model based on the work of Pross and Shaik is used to rationalize the computational results. The results obtained allow a number of predictions to be made.

I. Introduction

The deoxygenation of oxiranes to olefins is an important method in synthetic chemistry, and in proving structures (see eq 1). Various reagents have been used for this purpose over the last several decades.[1] In principle, the reaction may involve different pathways, depending on the nature of the reagent and the substrate. There may be a radical mechanism, via oxygen complexation or O−C bond insertion, or nucleophilic attack on the α- or β-carbon atom. The transformation may occur in one or several steps. Depending on the conditions applied, it may proceed stereospecifically with retention or inversion. In some cases there is a complete loss of stereochemistry.[1]

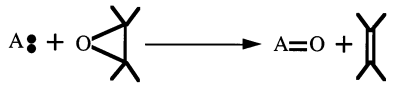

(1)

The deoxygenation of oxiranes with carbenes (CR_2) has been subject of wide-ranging investigations.[2−4] Recently, through the elegant studies performed by Lusztyk, Warkentin, and many co-workers,[2] it was found that singlet carbenes are capable of abstracting an oxygen atom from oxirane, undergoing the reaction as shown in eq 1 above. Several qualitative conclusions concerning the oxirane deoxygenation were obtained. (1) The magnitudes of the rate constants for oxygen atom transfer are dependent on the philicity of the carbene intermediate. (2) Trends in the kinetic data suggest that oxygen atom transfer occurs by a concerted mechanism through ylide-like transition states. (3) Ylides formed by the attack of carbenes on heteroatom donors were not actually observed for any of the heteroatom transfer reactions. (4) Absolute rate constants for the heteroatom transfer show that oxirane deoxygenation is a facile process.

It is these fascinating experimental results that inspire this study. If carbenes can be used as reagents for reductive deoxygenation of organic molecules, would it be possible to extend this to other heavier carbenes or carbene analogues? In this theoretical work, four heavy prototypical carbenes: silylene, SiH_2; germylene, GeH_2; stannylene, SnH_2; and plumbylene, PbH_2; were selected as model systems for investigation of their reaction mechanisms when each reacts with oxirane during an oxygen atom transfer reaction. For comparison, the simplest carbene species, methylene CH_2, has been studied in the present work as well.[4] Thus, in this study, five kinds of reactions, $XH_2 + OC_2H_4$ (X = C, Si, Ge, Sn, and Pb), were investigated using density functional theory (DFT). To the best of our knowledge, until now neither experimental nor theoretical studies have been performed on these systems, except for some carbenes and related reactive species.[2−4] Our purpose here is (1) to find potential carbene analogues that can facilitate the oxygen atom transfer reactions, (2) to ascertain whether such abstractions occur in a concerted fashion or in a stepwise biradical manner with a highly distorted transition state, (3) to predict trends in activation energies and reaction enthalpies, (4) to obtain a better understanding of the origin of barrier heights for such deoxygenation reactions, and (5) to provide experimentalists with a theoretical basis for predicting the relative reactivities of heavy carbenes.

II. Theoretical Methods

All geometries were fully optimized without imposing any symmetry constraints, although in some instances the resulting structure showed various elements of symmetry. For our DFT calculations, we used the hybrid gradient-corrected exchange functional proposed by Becke,[5] combined with the gradient-corrected correlation functional of Lee, Yang, and Parr.[6] This functional is commonly known as B3LYP, and has been shown to be quite reliable both for geometries and energies.[7] These B3LYP calculations were carried out using the Gaussian 94 program.[8] For consistency, the standard LANL2DZ basis sets were chosen for the carbon, hydrogen,[9] silicon, germanium, tin, and lead[10] atoms. We denote our B3LYP calculations by B3LYP/LANL2DZ. Vibrational frequency calculations at the B3LYP/LANL2DZ level were used to characterize all stationary points as either minima (the number of imaginary frequencies (NIMAG) = 0) or transition states (NIMAG = 1). The vibrational zero-point energy (ZPE, not scaled) corrections determined at the B3LYP/LANL2DZ level are also included, i.e., B3LYP/LANL2DZ + ZPE (B3LYP/LANL2DZ). Further

10.1021/jp021176l CCC: $22.00 © 2002 American Chemical Society
Published on Web 09/21/2002

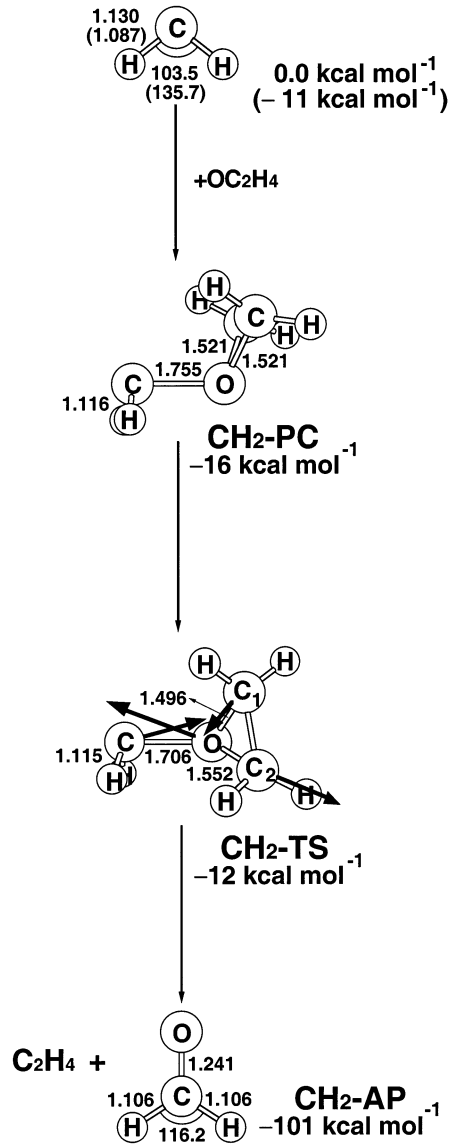

Figure 1. The B3LYP/LANL2DZ geometries (in ångstroms and degrees) for the precursor complexes (PC), transition states (TS), and abstraction products (AP) of oxirane with CH_2. The relative energies were obtained at the CCSD(T)/LANL2DZdp level of theory. Values in parentheses are in the triplet state. The heavy arrows indicate the main atomic motions in the transition state eigenvector.

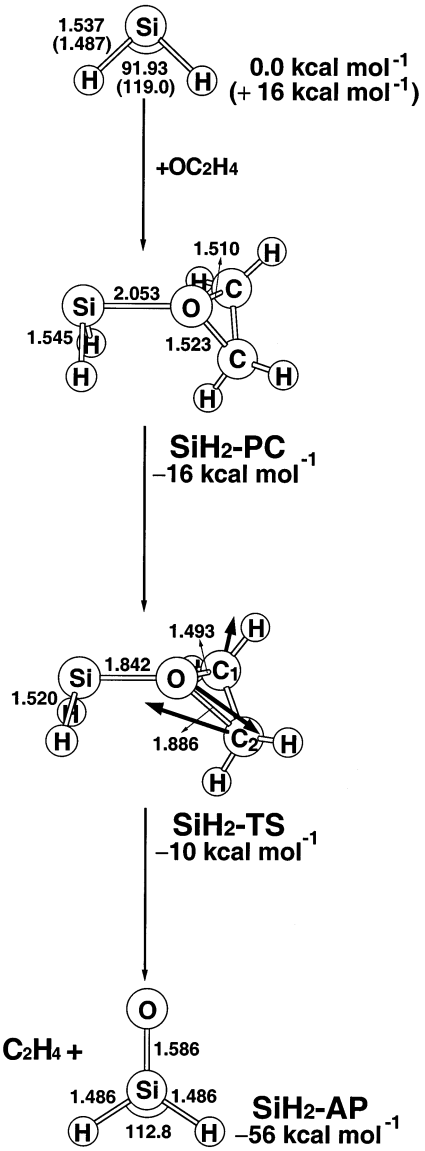

Figure 2. The B3LYP/LANL2DZ geometries (in ångstroms and degrees) for the precursor complexes (PC), transition states (TS), and abstraction products (AP) of oxirane with SiH_2. The relative energies were obtained at the CCSD(T)/LANL2DZdp level of theory. Values in parentheses are in the triplet state. The heavy arrows indicate the main atomic motions in the transition state eigenvector.

single-point CCSD(T) calculations were performed on all B3LYP optimized structures, i.e., CCSD(T)/LANL2DZdp//B3LYP/LANL2DZ + ZPE (B3LYP/LANL2DZ) (hereafter designed CCSD(T)).[11,12] All of the DFT and CCSD(T) calculations were performed using the GAUSSIAN 94 package of programs.[8]

III. Results and Discussion

In this section the results for four regions on the potential energy surfaces will be presented: XH_2 (X = C, Si, Ge, Sn, and Pb) + OC_2H_4, the precursor complex (PC), the transition state (TS), and the abstraction products (AP). The fully optimized geometries for those stationary points calculated at the B3LYP/LANL2DZ level are given in Figures 1−5, respectively. The relative energies at the B3LYP level of theory are collected in Table 1. Moreover, the optimized geometries of the compounds CH_2, SiH_2, and GeH_2 in the singlet state are collected in Table 2, together with some known experimental results.

A. Reactants. By analogy with all other known carbenes (CR_2), it is expected that the two lowest states of heavier carbene analogues (XH_2, X = Si, Ge, Sn, and Pb) are $^1A_1$ and $^3B_1$. These states are derived from the ground state HOMO, an essentially nonbonding σ orbital (a_1 symmetry) based on the X atom, and the LUMO, an effectively nonbonding p-π orbital (b_1 symmetry) on the X atom. As one can see in Figures 1−5, the triplet state of XH_2 has significantly wider bond angles (∠HXH) and shorter bond distances (X−H) than its closed shell singlet state. Indeed, this is usually the case in group 14 divalent compounds, in accordance with expectations of the Walsh rules.[13] Additionally, X−H bond distances for both singlet ($^1A_1$) and triplet ($^3B_1$) states show a monotonic increase down the group from C to Pb. Moreover, the singlet ∠HXH bond angles at the C, Si, Ge, Sn, and Pb centers in methylene, silylene, germylene, stannylene, and plumbylene, respectively, decrease, as expected, in the given order: 103° > 91.9° > 90.9° > 90.2° > 90.0°. However, the triplet ∠HXH bond angles follow a slightly different trend: 136° (C) > 119° (Si) ≈ 119° (Pb) > 118 (Ge) > 117° (Sn). These

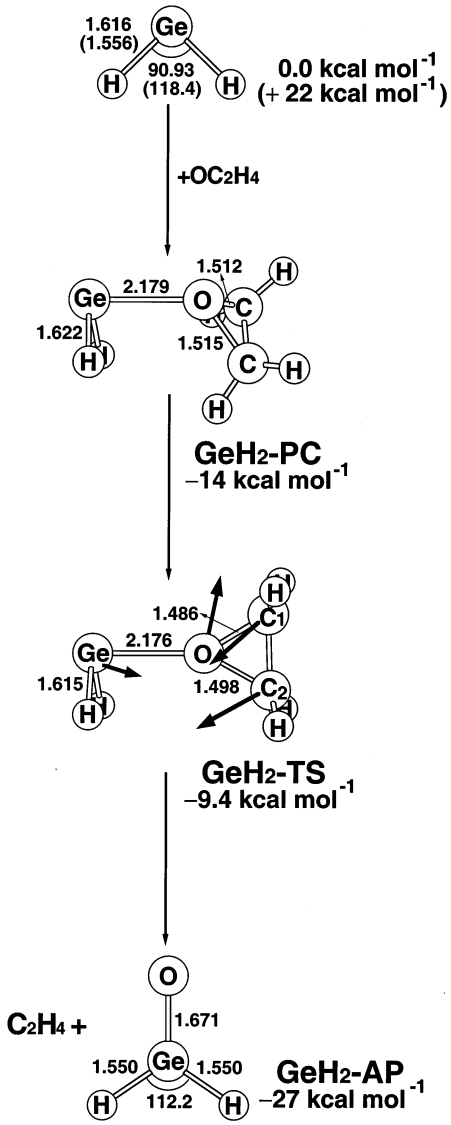

Figure 3. The B3LYP/LANL2DZ geometries (in ångstroms and degrees) for the precursor complexes (PC), transition states (TS), and abstraction products (AP) of oxirane with GeH_2. The relative energies were obtained at the CCSD(T)/LANL2DZdp level of theory. Values in parentheses are in the triplet state. The heavy arrows indicate the main atomic motions in the transition state eigenvector.

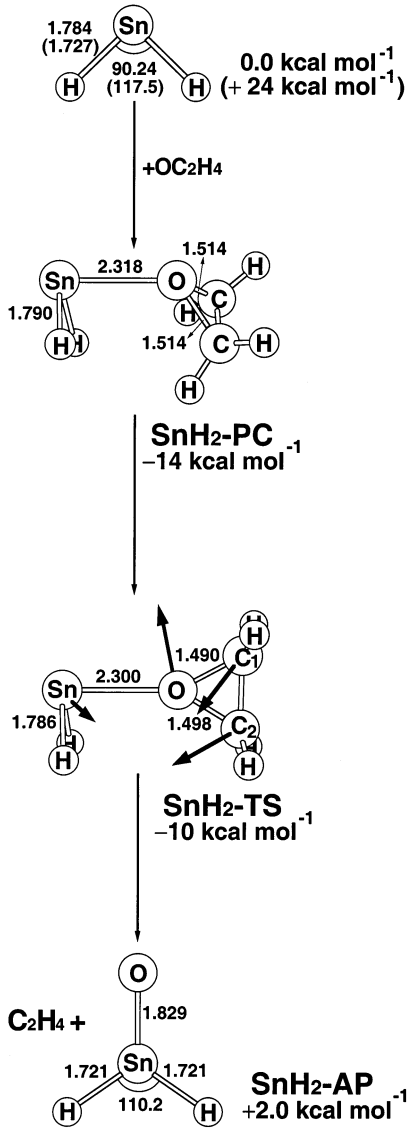

Figure 4. The B3LYP/LANL2DZ geometries (in ångstroms and degrees) for the precursor complexes (PC), transition states (TS), and abstraction products (AP) of oxirane with SnH_2. The relative energies were obtained at the CCSD(T)/LANL2DZdp level of theory. Values in parentheses are in the triplet state. The heavy arrows indicate the main atomic motions in the transition state eigenvector.

results are in good agreement with those obtained previously by Balasubramanian[14] for the case of singlet and triplet XH_2 species.

Furthermore, the singlet−triplet energy separations of group 14 dihdrides, namely, CH_2−PbH_2, have been the topics of many investigations for a number of years.[14−23] As often observed, the stability of the singlet state increases with decreasing electronegativity at the central atom in XH_2. That is to say, the singlet−triplet energy splitting generally increases as the atomic number of the central atom is increased. The reason for this may be partially due to the fact that the relativistic effect on a heavier central atom stabilizes the s orbital relative to the p, favoring the singlet state relative to the triplet.[24] This prediction is confirmed by our theoretical results as given in Table 1, i.e., an increasing trend in singlet−triplet energy splitting for CH_2 (−11 kcal/mol) < SiH_2 (16 kcal/mol) < GeH_2 (22 kcal/mol) < SnH_2 (25 kcal/mol) < PbH_2 (35 kcal/mol) at the CCSD(T) level of theory.[25,26] Again, these results are in qualitative agreement with those reported previously by several groups.[14−23] We shall use the above results to explain the origin of barrier heights for their oxygen atom transfer reactions in a later section.

B. Precursor Complexes. Before presenting our computational results for these abstraction reactions, it should be pointed out that experimental findings suggest that singlet state chemistry should be dominant because of the high reactivity of singlets toward heteroatom lone pairs.[2,3a] Therefore, our theoretical investigations for the heavy carbene abstractions will be confined to singlet potential energy surfaces from now on. As expected,[4] such oxygen atom transfer reactions may involve the formation of an initial precursor complex (PC). Thus, the geometries and energies of complexation of oxirane with carbene analogues, i.e., CH_2-PC, SiH_2-PC, GeH_2-PC, SnH_2-PC, and PbH_2-PC were also calculated. The optimized geometries are shown in Figures 1−5. For convenience, the energies are given relative to the reactant molecules, i.e., $XH_2 + OC_2H_4$, which are summarized in Table 1.

The closed-shell heavy carbene electron configuration is such that there is a vacant p orbital on the central atom X capable of

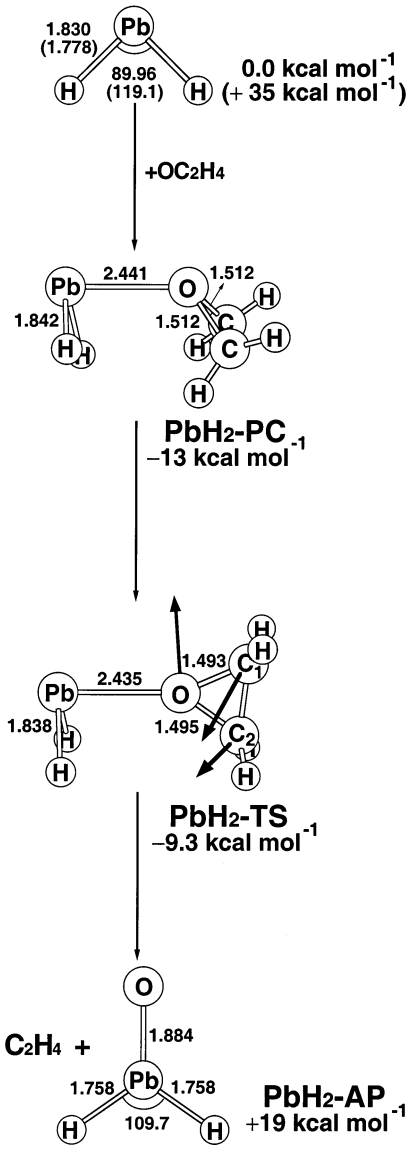

Figure 5. The B3LYP/LANL2DZ geometries (in ångstroms and degrees) for the precursor complexes (PC), transition states (TS), and abstraction products (AP) of oxirane with PbH_2. The relative energies were obtained at the CCSD(T)/LANL2DZdp level of theory. Values in parentheses are in the triplet state. The heavy arrows indicate the main atomic motions in the transition state eigenvector.

forming a chemical bond with a Lewis base, i.e., oxirane. As can be seen in Figures 1−5, these precursor complexes appear to have similar structures, in which optimal overlap between the lone pair orbital of OC_2H_4 and the empty p orbital of XH_2 is achieved by a parallel plane approach of the two molecules (see Scheme 1). The donor−acceptor interaction leads to calculated C−O, Si−O, Ge−O, Sn−O, and Pb−O bond distances of 1.75, 2.05, 2.18, 2.32, and 2.44 Å, respectively. This finding can be explained in terms of the size of the group 14 atom X, which should increase from C to Pb. Our attempt to locate molecular complexes at much longer X−O distances failed. Thus, our theoretical findings suggest that those complexes obtained in this work can be considered as Lewis acid−base adducts.

Furthermore, as can be seen from the data, our theoretical results suggest that stabilization energies for these five precursor complexes are within the range of −13 to −16 kcal/mol (at CCSD(T)). It should be noted that the precursor complex may dissociate, back to the initial recants, or cross the barrier to undergo another reaction before dissociation. As one can see in Table 1, their activation energies for the onward reaction are as follows: 4.2 (CH_2), 6.4 (SiH_2), 5.0 (GeH_2), 4.4 (SnH_2), and 3.8 kcal/mol (PbH_2) at the CCSD(T) level of theory. According to these computational results, it is therefore anticipated that experimental observations of these Lewis acid−base adducts formed during the reactions should be very difficult, since they are predicted to be kinetically unstable.

TABLE 1: Relative Energies for Singlet and Triplet Heavy Carbenes and for the Process Reactans → Precursor Complex → Transition State → Abstraction Products[a,b]

	system	ΔE_{st}[c] (kcal mol^{-1})	ΔE_{cpx}[d] (kcal mol^{-1})	$\Delta E^{\ddagger}$[e] (kcal mol^{-1})	ΔH[f] (kcal mol^{-1})
1	CH2	−11.12	−15.82	−11.64	−100.8
		(−18.07)	(−21.16)	(−17.58)	(−111.8)
2	SiH2	+15.78	−16.50	−10.05	−56.43
		(+13.76)	(−18.99)	(−14.78)	(−53.34)
3	GeH2	+22.14	−14.41	−9.371	−26.61
		(+22.46)	(−17.11)	(−13.94)	(−31.39)
4	SnH2	+24.48	−14.44	−9.985	+2.000
		(+25.98)	(−17.31)	(−14.70)	(−14.43)
5	PbH2	+35.30	−13.07	−9.296	+18.68
		(+36.80)	(−14.66)	(−12.05)	(+8.707)

[a] At the CCSD(T)/LANL2DZdp and B3LYP/LANL2DZ (in parentheses) levels of theory. The B3LYP optimized structures of the stationary points see Figures 1−5. [b] Energies differences have been zero-point corrected. See the text. [c] Energy relative to the corresponding singlet state. A positive value means the singlet is the ground-state. [d] The stabilization energy of the precursor complex, relative to the corresponding reactants. [e] The activation energy of the transition state, relative to the corresponding reactants. [f] The exothermicity of the product, relative to the corresponding reactants.

SCHEME 1

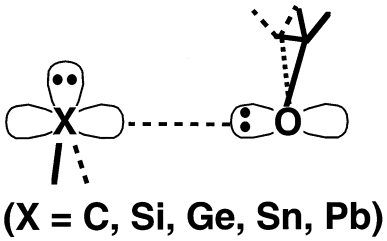

C. Transition States. The optimized transition state structures (CH_2-TS, SiH_2-TS, GeH_2-TS,SnH_2-TS, and PbH_2-TS) along with the calculated transition vectors are shown in Figures 1−5, respectively. The arrows in the figures indicate the directions in which the atoms move in the normal coordinate corresponding to the imaginary frequency. It is apparent that these transition states connect the corresponding precursor complexes (i.e., Lewis acid−base adducts) to the abstraction products. Examination of the single imaginary frequency for each transition state (237i cm^{-1} for CH_2-TS, 417i cm^{-1} for SiH_2-TS, 130i cm^{-1} for GeH_2-TS, 108i cm^{-1} for SnH_2-TS, and 98i cm^{-1} for PbH_2-TS) provides an excellent confirmation of the concept of an abstraction process. That is, the C−O bond stretches with the oxygen migrating to the central atom X of heavy carbene XH_2. These reactions appear to be concerted; we have been able to locate only one TS for each reaction and have confirmed that it is a true TS on the basis of frequency analysis.

A comparison of the five transition structures yields a number of trends. As seen in Figures 1−5, there is a dramatic effect on the intermolecular distances at the saddle points. Decreasing the electronegativity of the central atom X in the heavy carbene XH_2 causes a large increase in the H_2X-OC_2H_4 distance. That is, the newly forming X−O bond length increases in the order: CH_2-TS (1.71 Å) < SiH_2-TS (1.84 Å) < GeH_2-TS (2.18 Å) <

SnH_2-TS (2.30 Å) < PbH_2-TS (2.44 Å). In addition, the present calculations indicate that the greater the atomic weight of the central atom X, the less the asynchronicity of the oxygen-transfer reaction. For example, as shown in Figures 1−5, in CH_2 and SiH_2 cases one of the breaking bonds ($O-C_1$) is only slightly longer than in a normal O−C single bond of oxirane, while the other ($O-C_2$) is greatly stretched. On the other hand, two breaking bonds ($O-C_1$ and $O-C_2$) are nearly the same for the GeH_2, SnH_2, and PbH_2 abstraction reactions.

Moreover, the DFT calculations suggest that, the X=O double bond is stretched by 37%, 36%, 30%, 26%, and 30% for CH_2-TS, SiH_2-TS, and GeH_2-TS, SnH_2-TS, and PbH_2-TS, respectively, relative to their corresponding abstraction product H_2X=O. This strongly implies that, according to the Hammond postulate,[27] the transition state for a heavy carbene with a less electronegative central atom X should take on a more product-like character and the barrier should be encountered later than for a carbene analogue with a more electronegative central atom X. Our theoretical model calculations confirm this prediction. As demonstrated in Table 1, the barrier height (relative to the corresponding reactants) for the abstraction reaction follows a similar trend to the electronegativity of the central atom X: CH_2-TS (−12 kcal/mol) < SiH_2-TS (−10 kcal/mol) ≈ SnH_2-TS (−10 kcal/mol) < GeH_2-TS (−9.4 kcal/mol) < PbH_2-TS (−9.3 kcal/mol).

D. Abstraction Products. The optimized product structures (CH_2-AP, SiH_2-AP, GeH_2-AP, SnH_2-AP, and PbH_2-AP) are collected Figures 1−5 and the calculated reaction enthalpies for abstraction are given in Table 1. The expected products of the abstraction reactions of heavy carbenes with oxirane are ethylene as well as H_2X=O, the heavier element congener of a formaldehyde. To our knowledge, experimental structures for such compounds are not known as yet.[28,29] Again, as Figures 1−5 shows, the order of X=O bond length follows the same trend as the atomic weight of the central atom X: CH_2-AP (1.24 Å) < SiH_2-AP (1.59 Å) < GeH_2-AP (1.67 Å) < SnH_2-AP (1.83 Å) < PbH_2-AP (1.88 Å).

As mentioned earlier, a heavy carbene with a less massive but more elecronegative central atom reaches the transition state relatively early, whereas a carbene analogue with a more massive and less electronegative central atom arrives relatively late. The former is therefore predicted to undergo a more exothermic abstraction, which is borne out by our CCSD(T) calculations. For instance, the order of exothermicity follows the same trend as the activation energy: CH_2-AP (−101 kcal/mol) < SiH_2-AP (−56 kcal/mol) < GeH_2-AP (−27 kcal/mol) < SnH_2-AP (+2.0 kcal/mol) < PbH_2-AP (+19 kcal/mol). Note that the energetics of SnH_2-AP and PbH_2-AP are above those of their corresponding starting materials. This strongly indicates that the oxirane deoxygenations by stannylene and plumbylene are energetically unfavorable and would be endothermic. Namely, our theoretical findings suggest that the abstraction products of SnH_2 and PbH_2 are not produced from the oxygen atom transfer reaction of $SnH_2 + OC_2H_4 \rightarrow H_2Sn{=}O + C_2H_4$ and $PbH_2 + OC_2H_4 \rightarrow H_2Pb{=}O + C_2H_4$, respectively, but possibly exist if these compounds (H_2Sn=O and H_2Pb=O) are produced through other reaction paths.[28,29]

E. Theoretical Model for the Reaction Barrier. In this section, an intriguing model for interpreting the reactivity of heteroatom transfer reactions is provided by the so-called configuration mixing (CM) model, which is based on Pross and Shaik's work.[4,30] According to the conclusions of this model, the energy barriers governing processes as well as the reaction enthalpies should be proportional to the energy gap ΔE_{st} ($=E_{triplet} - E_{singlet}$) between the singlet and the triplet states of a heavy carbene XH_2. In other words, the smaller the ΔE_{st} of XH_2, the lower the barrier height and the larger the exothermicity and, in turn, the faster the abstraction reaction.

Bearing the above conclusion in mind, we shall explain the origin of the observed trends as shown previously in the following discussion:

Why is the oxirane deoxygenation of carbene analogue bearing a more electronegative central atom more facile than that of less electronegative central atom?

The reason for this can be traced back to the singlet−triplet energy gap (ΔE_{st}) of a six-valence-electron carbene. It is well established that a carbene with a more electronegative central atom should possess a smaller singlet−triplet splitting than one containing a less electronegative central atom.[31] In contrast to the carbenes, all silylenes, germylenes, stannylenes, and plumbylenes characterized to date have exclusively singlet ground states, with the energy of the singlet−triplet energy separation increasing with increasing atomic mass of the group-14 element,[32] which has been confirmed by our CCSD(T) calculations as given in Table 1. Furthermore, for the CCSD(T)/LANL2DZdp calculations on the aforementioned five systems, we obtain the following correlations (units in kcal/mol; r^2 is the correction coefficient):

$$\Delta E^{\ddagger} = 0.0516\Delta E_{st} - 11.0 \quad (r^2 = 0.908) \tag{1}$$

$$\Delta H = 2.63\Delta E_{st} - 78.1 \quad (r^2 = 0.918) \tag{2}$$

As one can see in eqs 1 and 2, there exists a linear correlation between ΔE_{st} and $\Delta E^{\ddagger}$ (the abstraction barrier) as well as ΔH (the reaction enthalpy). Consequently, our model calculations provide strong evidence that the electronic factor resulting from the group 14 element should play a decisive role in determining the reactivity of a heavy carbene.

IV. Conclusion

Taking all aforementioned five reactions ($XH_2 + OC_2H_4$) studied in this paper together, one can draw the following conclusions:

(1) We predict that the precursor complex might not exist in the course of the heavy carbene (XH_2) abstraction reaction.

(2) Oxirane undergoes concerted deoxygenation by reaction with CH_2 (singlet) and SiH_2 via an asynchronous four-center transition state. In contrast, GeH_2, SnH_2 and PbH_2 abstraction reactions are predicted to be concerted, but more synchronous, i.e., via a four-center transition structure with two more-or-less equal breaking bonds. As a result, their stereochemistry at the abstraction product (i.e., ethylene) is preserved.

(3) The reactivity of heavy carbenes (XH_2) toward the oxirane decreases with increasing atomic weight of the central atom X, i.e., in the order C > Si > Ge ≫ Sn > Pb. More specifically, *CH_2, SiH_2, and GeH_2 can readily abstract oxygen atoms from oxiranes, while SnH_2 and PbH_2 are unreactive with oxiranes*.

(4) Abstraction reactions with heavier carbenes (such as SnH_2 and PbH_2) are more endothermic (or less exothermic) than with CH_2, reflecting the weaker Sn=O and Pb=O vs C=O bond.

(5) If the heavier element congener of a formaldehyde is the primary product for heavy carbene abstraction reactions toward oxiranes, then the singlet−triplet splitting of a heavy carbene can be used as a diagnostic tool to predict the reactivities of various carbene analogues.

We encourage experimentalists to design new experiments to confirm our predictions.

Acknowledgment. The author would like to thank the National Center for High-Performance Computing of Taiwan for generous amounts of computing time and the National Science Council of Taiwan for their financial support. The author is also grateful to an anonymous referee for constructive comments.

References and Notes

(1) For reviews, see: (a) Bartok, M.; Lang, K. L., In *Small Ring Heterocycles*; Hassner, A. Eds.; Wiley: New York, 1985. (b) Adam, W.; Saha-Mîller, C. R.; Ganeshpure, P. A. *Chem. Rev*. **2001**, *101*, 3499.

(2) Pezacki, J. P.; Wood, P. D.; Gadosy, T. A.; Lusztyk, J.; Warkentin, J. *J. Am. Chem. Soc*. **1998**, *120*, 8681.

(3) (a) Wittig, G.; Schlosser, M. *Tetrahedron* **1962**, *18*, 1026. (b) Nozaki, H.; Takaya, H.; Noyori, R. *Tetrahedron Lett*. **1965**, 2563; (c) *Tetrahedron* **1966**, *22*, 3393. (d) Martin, M. G.; Ganem, B. *Tetrahedron Lett*. **1984**, 251. (e) Shields, C. J.; Schuster, G. B. *Tetrahedron Lett*. **1987**, 853. (f) Kovacs, D.; Lee, M.-S.; Olson, D.; Jackson, J. E. *J. Am. Chem. Soc*. **1996**, *118*, 8144.

(4) (a) Su, M.-D.; Chu, S.-Y. *Chem. Eur. J.* **2000**, *6*, 3777. (b) Su, M.-D.; Chu, S.-Y. *Chem. Phys. Lett.* **2000**, *320*, 475.

(5) (a) Becke, A. D. *Phys. Rev. A*, **1988**, *38*, 3098. (b) Lee, C.; Yang, W.; Parr, R. G. *Phys. Rev. B* **1988**, *37*, 785.

(6) Becke, A. D. *J. Chem. Phys*. **1993**, *98*, 5648.

(7) (a) Jursic, B.; Zdravkovski, Z. *J. Chem. Soc., Perkin Trans*. **1995**, 1223. (b) Jursic, B. *Chem. Phys. Lett*. **1996**, *256*, 603. (c) Jursic, B. *J. Mol. Struct. (THEOCHEM)* **1998**, *425*, 193. (d) Jursic, B. *J. Mol. Struct. (THEOCHEM)* **1998**, *452*, 145.

(8) Frisch, M. J.; Trucks, G. W.; Schlegel, H. B.; Gill, P. M. W.; Johnson, B. G.; Robb, M. A.; Cheeseman, J. R.; Keith, T.; Peterson, G. A.; Montgomery, J. A.; Raghavachari, K.; Al-Laham, M. A.; Zakrzewski, V. G.; Ortiz, J. V.; Foresman, J. B.; Cioslowski, J.; Stefanov, B. B.; Nanayakara, A.; Challacombe, M.; Peng, C. Y.; Ayala, P. Y.; Chen, W.; Wong, M. W.; Andres, J. L.; Replogle, E. S.; Gomperts, R.; Martin, R. L.; Fox, D. J.; Binkley, J. S.; Defrees, D. J.; Baker, J.; Stewart, J. P.; Head-Gordon, M.; Gonzalez, C.; Pople, J. A. Gaussian, Inc.: Pittsburgh, PA, 1995.

(9) Dunning, T. H.; Hay, P. J. *Modern Theoretical Chemistry*; Schaefer, H. F., Ed.; Plenum: New York, 1976; pp 1−28.

(10) (a) Hay, J. P.; Wadt, W. R. *J. Chem. Phys*. **1985**, *82*, 270; (b) *J. Chem. Phys*. **1985**, *82*, 284; (c) *J. Chem. Phys*. **1985**, *82*, 299.

(11) (a) Cizek, J. *Adv. Chem. Phys*. **1969**, *14*, 35. (b) Purvis, G. D.; Bartlett, R. J. *J. Chem. Phys.* **1982**, *76*, 1910. (c) Scuseria, G. E.; Schaefer, H. F., III *J. Chem. Phys*. **1989**, *90*, 3700.

(12) Check, C. E.; Faust, T. O.; Bailey, J. M.; Wright, B. J.; Gilbert, T. M.; Sunderlin, L. S. *J. Phys. Chem. A* **2001**, *105*, 8111.

(13) Gimarc, B. M., In *Molecular Structure and Bonding*; Academic Press: New York, 1979.

(14) Balasubramanian, K. *J. Chem. Phys.* **1988**, *89*, 5731.

(15) (a) Herzberg, G.; Johns, J. W. C., *Proc. R. Soc*., **1966**, *A292*, 107. (b) Petek, H.; Nesbitt, D. J.; Darwin, D. C.; Ogilby, P. R.; Moore, C. B.; Ramsay, D. A. *J. Phys. Chem*., **1992**, *96*, 1515.

(16) Dubois, I. *Can. J. Phys*. **1968**, *46*, 2485.

(17) Karolczak, J.; Harper, W. W.; Grev, R. S.; Clouthier, D. J. *J. Chem. Phys.* **1995**, *103*, 2839.

(18) Colvin, M.; Grev, R. S.; Schaefer, H. F., III; Bicerano, J. *Chem. Phys. Lett.* **1983**, *99*, 399.

(19) Mckellar, A. R.; W. Bunker; P. R.; Sears, T. J.; Evenson, K. M.; Saykally, R. S.; Langhoff, S. R. *J. Chem. Phys.* **1983**, *79*, 5251.

(20) Rice, J. C.; Handy, N. C. *Chem. Phys. Lett.* **1984**, *107*, 365.

(21) Balasubramanian, K.; McLean, A. D. *J. Chem. Phys.* **1986**, *85*, 5117.

(22) Phillips, R. A.; Buenker, R. J.; Beardsworth, R.; Bunker, P. R.; Jensen, P.; Kraemer, P. *Chem. Phys. Lett.* **1985**, *118*, 60.

(23) Berkowitz, J.; Greene, J. P.; Cho, H.; Ruscic, B. *J. Chem. Phys.* **1987**, *86*, 1235.

(24) (a) Pyykkî, P.; Desclaux, J.-P. *Acc. Chem. Res*. **1979**, *12*, 276. (b) Pyykkî, P. *Chem. Rev*. **1997**, *97*, 597.

(25) However, according to some experimental study, it is found that singlet−triplet energy splitting ($\Delta E_{st} = E_{triplet} - E_{singlet}$) for CH_2, SiH_2, and GeH_2 are −9.0 (see ref 26a), 21 (see ref 26b), and 27 (see ref 26c) kcal/mol, respectively.

(26) (a) Jensen, P.; Bunker, P. R. *J. Chem. Phys*. **1988**, *89*, 1327. (b) Berkowitz, J.; Greene, J. P.; Cho, H.; Ruscic, B. *J. Chem. Phys*. **1987**, *86*, 1235. (c) Karolczak, J.; Harper, W. W.; Grev, R. S.; Clouthier, D. J. *J. Chem. Phys.* **1995**, *103*, 2839.

(27) Hammond, G. S. *J. Am. Chem. Soc.* **1954**, *77*, 334.

(28) (a) Lin, C.-L.; Su, M.-D.; Chu, S.-Y. *J. Chem. Soc., Chem. Commun*., **1999**, 2383. (b) Lin, C.-L.; Su, M.-D.; Chu, S.-Y. *Chem Phys.* **1999**, *249*, 145.

(29) (a) Barrau, J.; Rina, G. *Coord. Chem. Rev.* **1998**, *178*, 593. (b) Power, P. P. *J. Chem. Soc., Dalton Trans.* **1998**, 2939. (c) Tokitoh, N.; Matsumoto, T.; Okazaki, R. *Bull. Chem. Soc. Jpn*. **1999**, *72*, 1665. (d) Robinson, G. H. *Acc. Chem. Res*. **1999**, *32*, 773. (e) Power, P. P. *Chem. Rev.* **1999**, *99*, 3463. (f) Leigh, W. J. *Pure Appl. Chem.* **1999**, *71*, 453. (g) Tokitoh, N. *Pure Appl. Chem.* **1999**, *71*, 495. (h) Okazaki, R.; Tokitoh, N. *Acc. Chem. Res.* **2000**, *33*, 625.

(30) (a) Shaik, S. *J. Am. Chem. Soc*., **1981**, 103, 3691. (b) Shaik, S.; Schlegel, H. B.; Wolfe, S., *Theoretical Aspects of Physical Organic Chemistry*; John Wiley & Sons. Inc.: New York, 1992. (c) Pross, A. *Theoretical and Physical principles of Organic Reactivity*; John Wiley & Sons, Inc.; New York, 1995.

(31) (a) Carter, E. A.; Goddard, W. A., III *J. Phys. Chem.* **1986**, *90*, 998; (b) *J. Phys. Chem.* **1987**, *91*, 4651; (c) *J. Chem. Phys*. **1988**, *88*, 1752. (d) Shin, S. K.; Goddard, W. A., III.; Beauchamp, J. L. *J. Phys. Chem.* **1990**, *94*, 6963. (e) Irikura, K. K.; Goddard, W. A., III.; Beauchamp, J. L. *J. Am. Chem. Soc*. **1992**, *114*, 48.

(32) Apeloig, Y. *The Chemistry of Organic Silicon Compounds*; Patai, S., Rappoport, Z., Eds.; Wiley: Chichester, 1998; Part I, pp 57−225.